International Journal of Innovative Computing, Information and Control
Volume **9**, Number **3**, March **2013**

 ISSN 1349-4198
pp. 1211–1231

WIDE AREA ROBUST CENTRALIZED PSO-BASED SPECIFIED STRUCTURE H_∞ POWER SYSTEM DAMPING CONTROLLER DESIGN CONSIDERING UNCERTAINTIES IN TIME DELAY AND SYSTEM PARAMETERS

Issarachai Ngamroo

School of Electrical Engineering
Faculty of Engineering
King Mongkut's Institute of Technology Ladkrabang
Bangkok 10520, Thailand
knissara@kmitl.ac.th

Received January 2012; revised May 2012

Abstract. *It is well known that the time delay due to the wide area phasor measurement may cause a malfunction of wide area centralized control of power system damping controller (PSDC) and system instability eventually. Nevertheless, the uncertainties due to time delay and system parameters have never been considered in the previous researches of PSDC design. To tackle this problem, a wide area robust centralized particle swarm optimization (PSO)-based specified structure H_∞ PSDC design taking uncertainties due to communication delay and system parameters into account is proposed in this paper. Without explicit mathematic equations, the inverse input multiplicative model is applied to represent the unstructured uncertainties. The structure of PSDC is the practical 2nd order lead/lag compensator. To automatically tune the control parameters, the optimization based on an enhancement of damping effect and robust stability margin is achieved by PSO. To evaluate the proposed design technique, two examples of robust centralized PSDC, i.e., power system stabilizer and thyristor control series capacitor are demonstrated in a two-area four-machine interconnected power system. Simulation study confirm that the proposed robust centralized PSDC is much superior to the conventional centralized PSDC in terms of stabilizing effect and robustness against uncertainties due to time delay and system parameters.*

Keywords: Wide area monitoring system, Phasor measurement unit, H_∞ control, Time delay, System uncertainties, Power system stability, Particle swarm optimization

1. **Introduction.** At present, the electric power consumptions, severe faults and the interconnections among power systems with long tie-line increase considerably. In addition, renewable energy sources with intermittent power generation such as wind and solar tend to penetrate to power systems significantly. These factors mainly cause the severe problem of wide area power oscillations with poor damping [1,2]. In the worst case of the undamped power oscillation, the system may be unstable. As a result, the cascade tripping will occur and result in the partial or complete blackout.

To tackle the power oscillation problem, the power system damping controllers (PSDC) such as automatic voltage regulator (AVR), power system stabilizer (PSS), thyristor series controlled capacitor (TCSC) and flexible AC transmission systems (FACTS) devices, have been applied. In [3], the robust AVR design based on mixed H_2/H_∞ pole placement using linear matrix inequality has been proposed. In recent research, a novel technique for designing decentralized stabilizers for robust control in power systems using an H_∞ criterion has been presented. In [4], the nonlinear robust controller design for TCSC has been studied. These proposed PSDCs have successfully solved the local oscillation

problem. Nevertheless, these PSDCs use the local signal as the controller input. They may fail to stabilize the wide area power oscillations. The PSDCs which use the wide area signals as the controller input for wide area stabilization, are highly expected.

Recently, the phasor measurement units (PMUs) which are synchronized based on the time stamp of the global positioning system (GPS) have been proposed [5]. The application of GPS-synchronized PMUs for wide area monitoring and control system has been presented [6]. In addition, it can be applied to wide area stabilizing control by PSDC such as PSS and FACTS devices [7]. Nevertheless, these proposed PSDCs have not considered the time delay effect of PMU data transfer due to communication. This may cause the malfunction of PSDC and system instability finally. Besides, not only in power system control, it has been proved in many research areas that the time delay significantly affects the system stability.

To handle this problem, many research works have proposed a wide area PSDC design considering time delay. In [8], the wide area PSS considering time delay effect has been presented. In [9], the wide area measurements-based two-level control design considering signal transmission delay has been proposed. Besides, the time delay compensation of a wide area measurements-based hierarchical voltage and speed regulator has been studied in [10]. Even in other research areas, the time delay has also been taken into account in the control design. In recent research, the stabilization for a class of uncertain multi-time delays system using sliding mode controller has been presented. And, the observer based model reference output feedback tracking control for switched linear systems with time delay has been proposed. Also, the neural network robust adaptive control for a class of time delay uncertain nonlinear systems has been studied. However, the controllers in [8-10] or previous works have never considered uncertainties due to time delay and system parameters variation; the robust stability of these controllers cannot be guaranteed in the face of several uncertainties.

To enhance the robustness against system uncertainties due to system parameters variation, the H_∞ control has been applied to many researches. In [11], the H_∞ robust controller design of media advance systems with time domain specification has been presented. The state feedback H_∞ control for networked control systems has been studied. Besides, the network-based H_∞ control of systems with time-varying sampling period has been proposed. Nevertheless, the controllers in [11] still have a high order. Therefore, it is difficult to realize in practical systems. Furthermore, the uncertainty due to time delay is still the remaining problem for the robust controller design.

To overcome the high order problem of H_∞ controller, the fixed structure H_∞ controllers have been proposed. For example, the design and implementation of a high performance hard disk serve motor using genetic algorithm based 2DOF robust controller has been presented. Also, the heuristic based automatic weight selection and fixed structure robust loop shaping control for power system control applications has been studied. In [12], the weight optimization and structure specified robust H_∞ loop shaping control of a pneumatic servo system using genetic algorithm has been proposed. Although the proposed controllers in these literatures provide satisfactory damping effect, the weighting functions selection is still an evitable problem in the design process. The robust control design without difficulty of weighting functions selection is highly expected.

To achieve the controller with practical structure, low order and high robustness against uncertainties due to time delay and system parameters without the weighting functions selection, this paper proposes a new wide area robust centralized based specified structure H_∞ PSDC. Without exact mathematical model, the inverse input and output multiplicative perturbations is applied to represent unstructured uncertainties due to time delay and system parameters. The PSDC structure is specified as the practical 2nd order lead/lag

compensator. The PSDC parameters are automatically tuned based on an enhancement of robust stability and damping performance by particle swarm optimization (PSO). Two examples of PSDC, i.e., PSS and TCSC designed by the proposed method are shown in a two-area four-machine interconnected power system. Simulation study confirms that the proposed PSDC is much superior to the conventional PSDC in terms of stabilizing effect and robustness against time delay and system uncertainties.

2. Proposed Wide Area Robust Centralized PSDC Design.

2.1. System modeling. The two-area four-machine interconnected power system [2] as shown in Figure 1 is used as the study system to explain the proposed control design. Both areas are connected by an AC tie-line and exhibit an inter-area oscillation mode with weak damping. The electric power (P_{tie}) flows from area 1 to 2. Each generator is represented by the 6th order state model with 1st order transfer function of AVR and governor. It is assumed that the PSDC$_i$ ($i = 1, 2, \ldots, m$) and stabilizing device$_i$ ($i = 1, 2, \ldots, m$) such as PSS and FACTS controllers, are located in the system. Four PMUs synchronized by GPS are located at the terminal bus of generators G1, G2, G3 and G4. The speed deviations of G1 to G4 ($\Delta\omega_{G1}$, $\Delta\omega_{G2}$, $\Delta\omega_{G3}$ and $\Delta\omega_{G4}$) are measured by PMUs and transferred to the control center with the received time delay τ_{d1}. After the control processing of PSDC$_i$ at the control center, the ith control signal (Δu_i,) from the control center is sent to the ith stabilizing device in the system with the transmitted time delay τ_{d2}. In this work, it is assumed that the data transfer is performed by a fiber-optic cable which has about 50 ms of time delay for one way communication [13].

The power system in Figure 1 can be represented by the feedback control system included with both time delays as depicted in Figure 2. $G(s)$ is the transfer function of power system. $K(s)$ is the transfer function of centralized PSDC located at the control

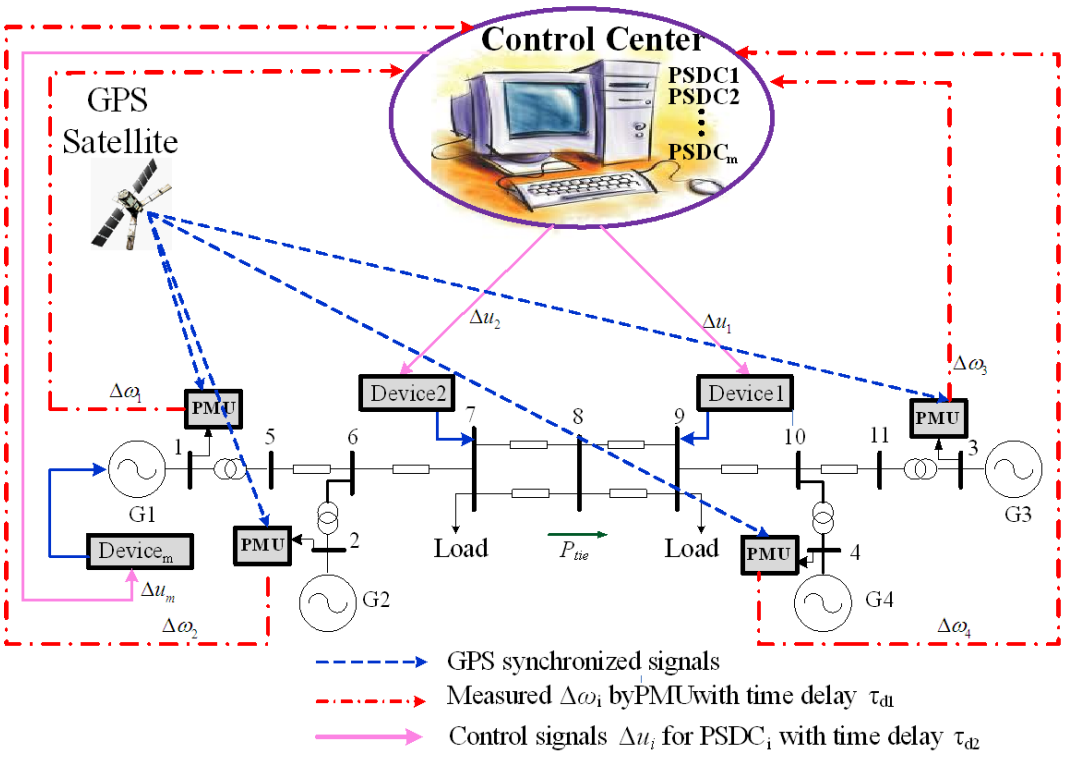

FIGURE 1. Concept of the proposed design

center which is defined by

$$K(s) = \begin{bmatrix} K_{PSDC1}(s) & 0 & 0 & 0 & 0 & 0 \\ 0 & K_{PSDC2}(s) & 0 & 0 & 0 & 0 \\ 0 & 0 & \ddots & 0 & 0 & 0 \\ 0 & 0 & 0 & K_{PSDCi}(s) & 0 & 0 \\ 0 & 0 & 0 & 0 & \ddots & 0 \\ 0 & 0 & 0 & 0 & 0 & K_{PSDCm}(s) \end{bmatrix} \tag{1}$$

where $K_{PSDCi}(s)$, $i = 1, \ldots, m$ are the ith PSDC and m is the number of PSDCs. The superscript T is the transpose of matrix.

The PSDC structure consists of a washout high-pass filter, a stabilizer gain, a phase-compensation and an output limiter as depicted in Figure 3. The input signal is the speed deviation of the ith generator ($\Delta\omega_i$) measured by PMU. The washout high-pass filter with time constant T_w eliminates low frequencies which are embedded in the $\Delta\omega$ signal. Here, T_w is set at 10.0. Besides, the phase compensation is the 2nd order lead/lag structure where K_{Si} are controller gains and T_{i1}, T_{i2}, T_{i3} and T_{i4} are time constants. The output signal is Δu_i. All parameters are optimized by the proposed method.

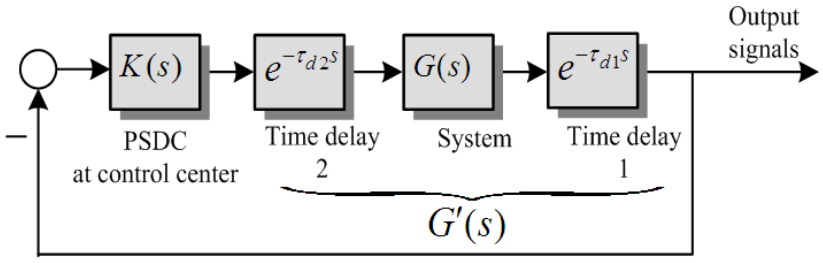

FIGURE 2. Feedback control system with time delay

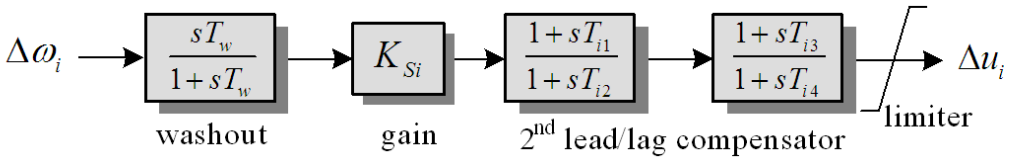

FIGURE 3. Structure of $K_{PSDCi}(s)$

The state equation of power system can be expressed as

$$\dot{x} = Ax + Bu \tag{2}$$

$$y = Cx \tag{3}$$

where x is state variable, u and y are input and output of system.

As shown in Figure 2, the time delay effect can be represented by $e^{-\tau_d s}$, where τ_d is time delay. Here, the time delay term is represented by Pade's approximation as

$$e^{-\tau_d s} \approx \left(1 - \frac{\tau_d}{2}s\right) \Big/ \left(1 + \frac{\tau_d}{2}s\right) \tag{4}$$

Equation (4) can be rewritten in state space equation by

$$\dot{x}_d = A_d x_d + B_d u_d \tag{5}$$

$$y_d = C_d x_d + D_d u_d \tag{6}$$

where x_d, u_d and y_d are state variable, input and output of time delay term, respectively.

The power system equation and time delay term can be combined to be the state equation of system included with time delay as

$$\dot{x}_t = \bar{A}x_t + \bar{B}u_t \tag{7}$$

$$y_t = \bar{C}x_t \tag{8}$$

where

$$\bar{A} = \begin{bmatrix} A & BC_{\tau_{d2}} & 0 \\ 0 & A_{\tau_{d2}} & 0 \\ B_{\tau_{d2}}C & 0 & A_{\tau_{d1}} \end{bmatrix}, \quad \bar{B} = \begin{bmatrix} BD_{\tau_{d2}} \\ B_{\tau_{d2}} \\ 0 \end{bmatrix}, \quad \bar{C} = \begin{bmatrix} D_{\tau_{d1}}C & 0 & C_{\tau_{d1}} \end{bmatrix} \tag{9}$$

Equations (7) and (8) can be represented by the transfer function by $G'(s)$ as indicated in Figure 2. Here, $G'(s)$ is defined as the nominal plant model included with the time delay. To simplify the parameters optimization of centralized PSDC, the balanced realization is applied to reduce the order of the system. The appropriate reduced order is considered by Hankel Singular Value (HSV) [14]. The reduced nominal plant model is referred to as $G'_R(s)$.

2.2. **Robust control design considering time delay uncertainty.** Since the communication delay and system operating conditions can be varied from the normal operating point, these unstructured uncertainties can be represented by Δ_{M1} and Δ_{M2} at the input and output of $G'_R(s)$ as shown in Figure 4, respectively. Δ_{M1} and Δ_{M2} are defined as the inverse multiplicative input and output perturbations, respectively [15]. Detail of mathematical derivation of this model is given in Appendix. Note that without exact mathematical expressions, this uncertainty model is able to represent all possible uncertainties in the system. Based on the small gain theorem, the robust stability condition against all possible system uncertainties is given by

$$\left\| 1 + K(s)[I - \Delta_{M1}]^{-1} \left\{ e^{-T_{d1}s} G(s) e^{-T_{d2}s} \right\} [I - \Delta_{M2}]^{-1} \right\|_\infty > 0 \tag{10}$$

Then

$$\|\Delta_t\|_\infty < \frac{1}{\|I + L(s)\|_\infty^{-1}} \tag{11}$$

where Δ_t is the total system uncertainties: $(\Delta_t = \Delta_{M1} + \Delta_{M2} - \Delta_{M1}\Delta_{M2})$ and $L(s) = K(s)\left\{e^{-T_{d1}s}G(s)e^{-T_{d2}s}\right\}$.

The right hand side of (11) implies the size of system uncertainties or the robust stability margin against uncertainties. By minimizing $\|1 + L(s)\|_\infty^{-1}$, the robust stability margin of

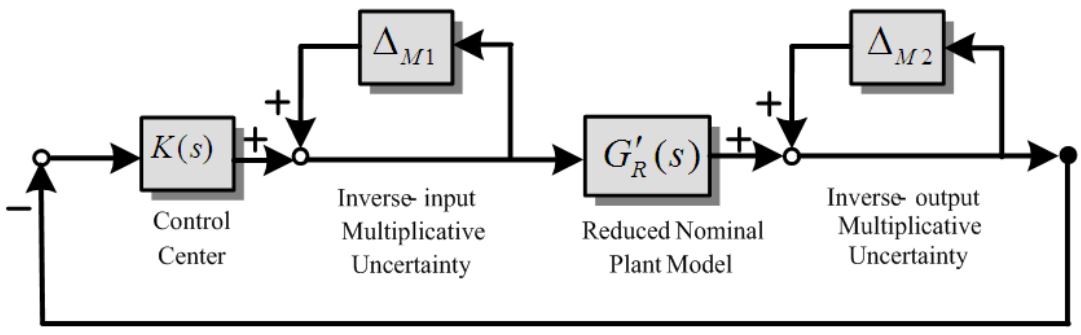

FIGURE 4. Feedback control system with inverse input and output multiplicative perturbations

the closed-loop system becomes maximum. This concept can be applied to formulate the optimization problem as

$$\begin{array}{ll} \text{Minimize} & \|1+L(s)\|_{\infty}^{-1} \\ \text{Subject to} & \zeta \geq \zeta_{spec}, \quad \sigma \geq \sigma_{spec}, \\ & K_{i,\min} \leq K_i \leq K_{i,\max}, \quad T_{ij,\min} \leq T_{ij} \leq T_{ij,\max}, \\ & i=1,\ldots,m, \quad j=1,\ldots,4 \end{array} \tag{12}$$

where $\|\|_{\infty}$ is the infinite norm of transfer function, ζ and ζ_{spec} are the actual and desired damping ratio of the dominant inter-area modes, respectively; σ and σ_{spec} are the actual and desired real part of the eigenvalue corresponding to the dominant modes; $K_{i,\max}$ and $K_{i,\min}$ are the maximum and minimum controller gains, respectively; $T_{ij,\max}$ and $T_{ij,\min}$ are the maximum and minimum time constants, respectively. The optimization objective is not only to improve the robustness of the controller but also to move the dominant inter-area modes to the D-stability region as illustrated in Figure 5. This optimization problem is solved by PSO [16].

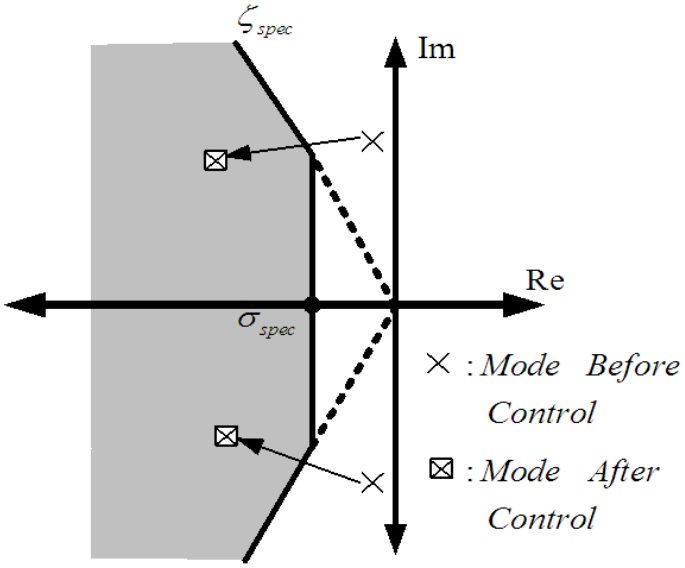

FIGURE 5. D-stability region

The PSO was discovered through simulation of a simplified social model, where each population is called a swarm [16]. In PSO, multiple solutions collaborate simultaneously. Each candidate, called a particle, flies through problem space to look for the optimal position, similar to food searching of bird swarm. A particle adapts its position based on its own knowledge, and knowledge of neighboring particles. The algorithm is initialized with a population of random particles. It searches for the optimal solution by updating particles in generations. The PSO has been applied to many optimization problems. In [17], the kernel principal component analysis and multi-class support vector machine based on PSO have been applied to power quality problem classification. Figure 6 depicts the flowchart of PSO algorithm.

The PSO algorithm is briefly explained as follows:

1) Specify the parameters of PSO. Initialize a population of the particles with random positions and velocities.
2) Evaluate the objective function in (12) for each particle.

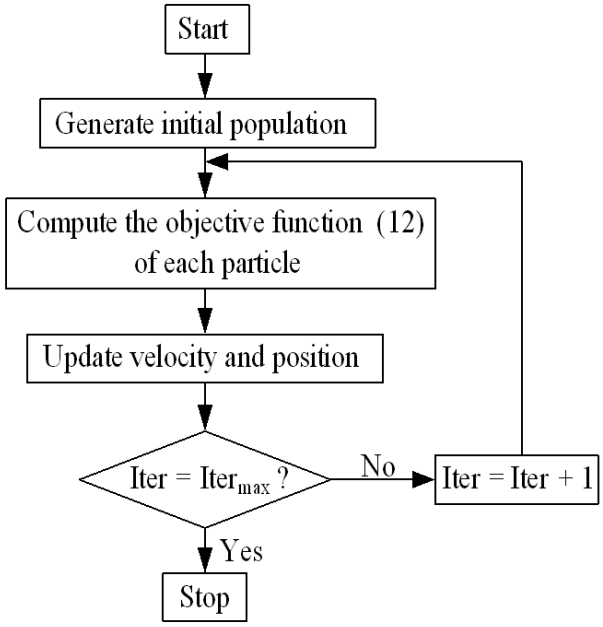

FIGURE 6. Flowchart of PSO algorithm

3) Compare the fitness value of each particle with its best position for particle (*pbest*). The best fitness value among all *pbests* is the best position of all particles in the group (*gbest*).
4) Update the velocity v_i and position of particle x_i by

$$v_{i+1} = w.v_i + c_1.rand_1.(pbest - x_i) + c_2.rand_2.(gbest - x_i) \tag{13}$$

$$x_{i+1} = x_i + v_{i+1} \tag{14}$$

$$w = w_{\max} - \frac{w_{\max} - w_{\min}}{iter_{\max}} iter \tag{15}$$

where c_1 and c_2 are the cognitive and social acceleration factors, respectively. $rand_1$ and $rand_2$ are the random numbers of range $(0, 1)$. w is the inertia weight factor. $w_{\min}$ and $w_{\max}$ are the minimum and maximum of inertia weight factors, respectively. *iter* and $iter_{\max}$ are the iteration count and maximum iteration, respectively.
5) When the maximum number of iterations is arrived, stop the process. Otherwise go to step 2.

The true significance and novel contribution of the proposed robust control design which has never been presented in the previous works, can be emphasized as follows.

1) The proposed robust control design is carried out in the system model considering uncertainties due to both time delay and system parameters variation. Without exact mathematic equations, the inverse input and output multiplicative perturbations have been applied to represent all possible unstructured uncertainties in the proposed model. This developed model not only simplifies the representation of system uncertainties, but also makes the control design practically and conveniently.
2) In contrast to a conventional H_∞ controller which has a high order, the designed robust PSDC is specified as the 2nd order lead/lag compensator which is easy to realize in practical systems. Besides, the controller structure may be specified as other structures such as PI and PID. Irrespective of the controller structure, the high

robustness and damping performance of the designed controller can be guaranteed by the proposed optimization.

3) Without difficulty of weighting function selection like conventional H_∞ controllers [11] and fixed structure H_∞ loop shaping controllers [12], the controller parameters of the proposed PSDC can be automatically optimized based on (12) by PSO.
4) The proposed robust PSDC with 2nd order and single input signal can be readily implemented in practical systems. Moreover, it is very robust against system uncertainties due to variation of time delays, several system operating conditions and severe disturbances.

The application of the proposed method can be described as follows.

1) The proposed PSDC can be applied to robustly stabilize wide area power oscillation in large scale interconnected power systems against system uncertainties such as operating conditions, time delay, severe disturbances and system parameters variation.
2) The proposed control method can be applied to design a robust PSDC with any specified structure such as PI, PID and lead/lag compensator.
3) The proposed control method can be applied to design a PSDC of any power stabilizing devices such as power system stabilizer, flexible ac transmission system devices and high-voltage direct current transmission system.
4) The proposed control method can be applied not only to power system control area, but also to other control systems such as a position control of a one-link manipulator under input time delay, the robust high-voltage direct current stabilizing control using wide area measurement [19], the robust H_∞ power control for CDMA cellular communication systems [20], a delay-dependent dual-rate PID controller over and ethernet network [21] and robust control of networked control systems with random time delays in both forward and backward communication links [22].

3. **Application 1: Wide Area Robust Centralized PSS Design.** The first application of the proposed method is to design the robust centralized PSSs as PSDCs as shown in Figure 7. Each generator (G1, G2, G3 and G4) is equipped with AVR which is used to maintain the terminal voltage (V_{t1}, V_{t2}, V_{t3}, V_{t4}). The control signals (Δu_1, Δu_2, Δu_3, Δu_4) from PSS1 to PSS4 are sent from the control center to AVR1 to AVR4 of G1 to G4, respectively. Totally there are 20 parameters for PSS1 to PSS 4. These parameters are simultaneously optimized by the proposed method.

The order of the overall system $G'(s)$ is 40. After the model reduction by HSV, Figure 8 shows the order of reduced system versus the normalized HSV (σ_i/σ_1) where σ_1 and σ_i are the HSV of the 1st and ith order of the reduced system. As suggested in [14], the appropriate reduced order is a user specified quantity that determines the trade-off between accuracy and complexity. The accuracy of the reduced order system can be evaluated by comparing the frequency response between the full order and reduced order system from the plot of singular values. Here, the normalized HSV is set at 5×10^{-4}. Consequently, the appropriate order of the reduced model is 21. The reduced nominal plant model is referred to as $G'_R(s)$. As shown in Table 1, the eigenvalues corresponding to the inter-area oscillation mode of the reduced order 21th system and the full order system have almost the same values. Besides, the plots of singular values of 21th order system and the full order system are illustrated in Figure 9. The peak resonance of all plots occurs at about 4 rad/s. This frequency is consistent with the imaginary part of the eigenvalue. Here, the 21th order system is chosen as the model for PSS parameters optimization.

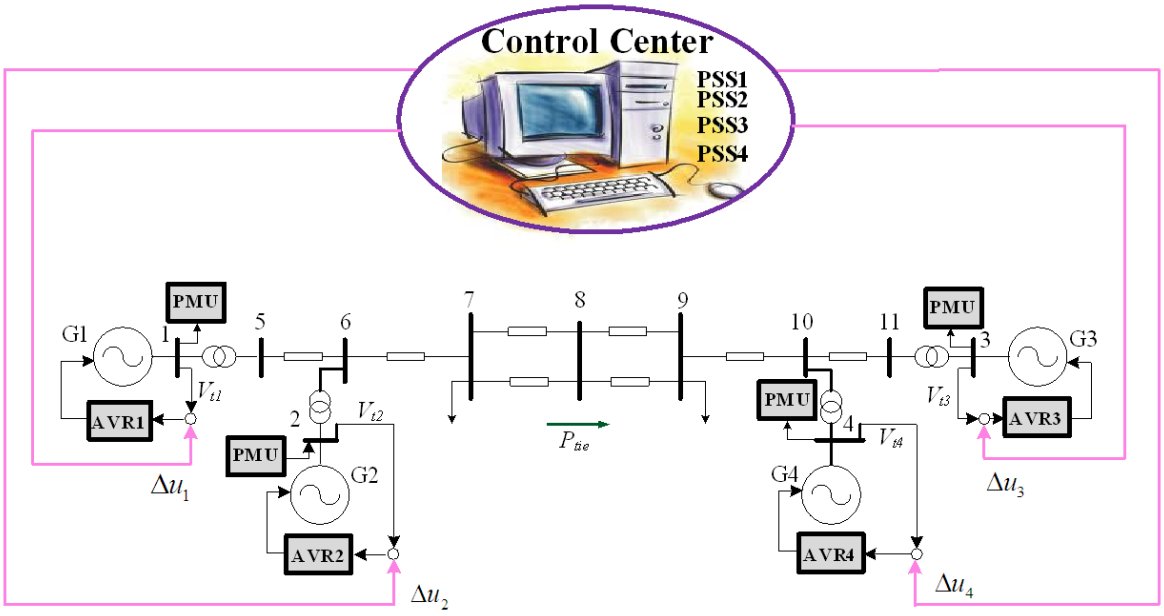

FIGURE 7. Wide area stabilization by PSS

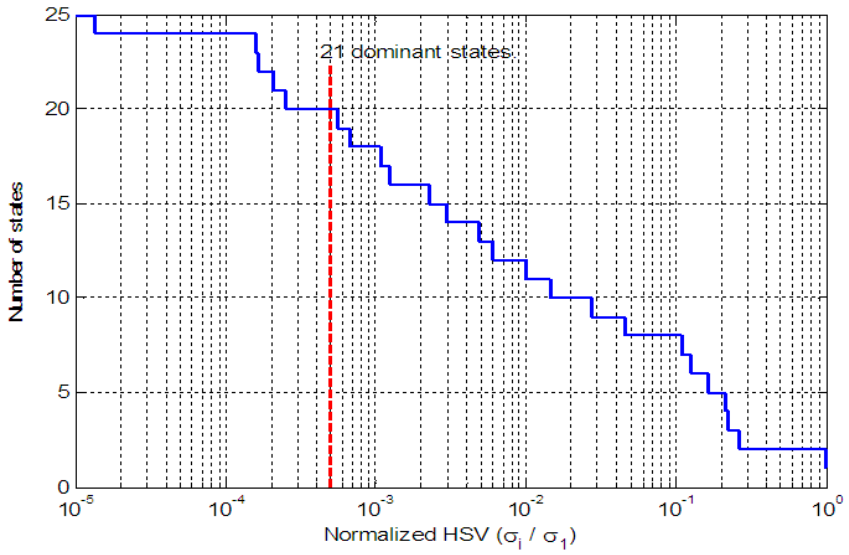

FIGURE 8. The order of reduced system relative to the normalized HSV

TABLE 1. Comparison of eigenvalues of inter-area mode between reduced and full order systems

Type of model	Oscillation Mode	Eigenvalue	Damping ratio	Frequency (Hz)
21th order	Inter-area	$-0.0629 \pm 3.9884i$	0.0158	0.6348
	Local 1	$-0.8626 \pm 6.9946i$	0.1224	1.1132
	Local 2	$-0.8610 \pm 7.2192i$	0.1184	1.1490
Full order	Inter-area	$-0.0629 \pm 3.9884i$	0.0158	0.6348
	Local 1	$-0.8625 \pm 6.9943i$	0.1224	1.1132
	Local 2	$-0.8609 \pm 7.2188i$	0.1184	1.1489

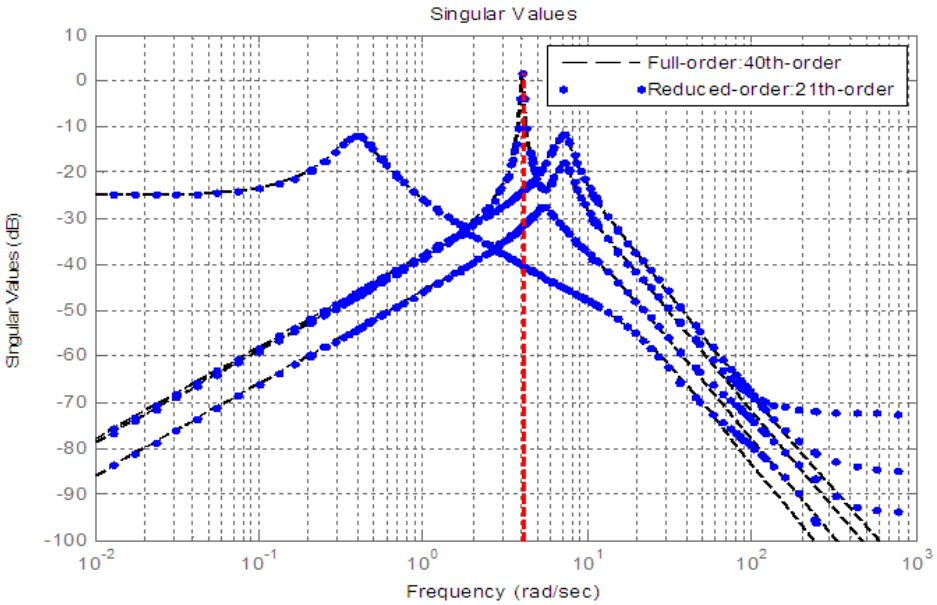

FIGURE 9. Singular values of full order and reduced order systems

TABLE 2. Operating conditions (100 MVA base)

Case	Event	Network structure	P_{tie} (p.u.)
1	A 3 phase fault occurs at one line between bus 7 and 8 at time = 2.0 s, The faulted line is opened at time = 2.07 s and not re-closed.	No change	3.5
2	A temporary 3 phase fault at bus 6 at time = 2.0 s for 75 ms. The fault is cleared.	One line between bus 7 and 8 is opened	4.5
3	One line between bus 7 and 8 is opened at time = 2.0 s and not re-closed.	No change	4.8

For parameters optimization by PSO, the design specification and range of search parameters are set as follows: $\zeta_{spec} = 0.05$, $\sigma_{spec} = -0.1$, $K_{i,\min} = 1.0$, $K_{i,\max} = 25$, $T_{i(1,2),\min} = 0.01$, $T_{i(1,2),\max} = 0.1$, $T_{i(3,4),\min} = 1$, $T_{i(3,4),\max} = 10$, number of particles = 24, maximum iterations = 100, acceleration factors = 2, and the minimum and maximum inertia weights are set at 0.4 and 0.9, respectively. The PSO is carried out based on the normal operating condition in case 1 as described in Table 2. As a result, the robust centralized controllers of PSS which is referred to as "RPSS", are obtained as

$$\begin{aligned}
\text{RPSS:} \quad K_{RPSS,G1}(s) &= 15.7380\frac{(1+0.0696s)}{(1+0.0100s)}\frac{(1+3.7297s)}{(1+3.4940s)} \\
K_{RPSS,G2}(s) &= 18.8819\frac{(1+0.0568s)}{(1+0.0109s)}\frac{(1+2.7048s)}{(1+5.3720s)} \\
K_{RPSS,G3}(s) &= 18.6350\frac{(1+0.0734s)}{(1+0.0107s)}\frac{(1+2.5992s)}{(1+7.7281s)} \\
K_{RPSS,G4}(s) &= 14.6234\frac{(1+0.0709s)}{(1+0.0157s)}\frac{(1+1.7084s)}{(1+6.5259s)}
\end{aligned} \tag{16}$$

The robustness of RPSS is compared with the conventional PSS designed without considering the time delay and robustness which is referred as "CPSS" [2]. The CPSS of each generator is obtained as

$$\text{CPSS} \qquad K_{CPSS}(s) = 20.00\frac{(1+0.05s)}{(1+0.02s)}\frac{(1+3.00s)}{(1+5.40s)} \tag{17}$$

The eigenvalue and damping ratio of local and inter-area oscillation modes of CPSS and RPSS as described in Table 3. Without PSS, the damping ratio of oscillation mode is very poor. On the other hand, the damping ratio is improved by CPSS. For RPSS, the damping ratio and the real part of oscillation modes are achieved as the desired specification.

Nonlinear simulation studies of three case studies as in Table 2 are carried out to evaluate the performance and robustness of CPSS and RPSS.

Comparisons of speed difference between generators 3 and 1 which represent the inter-area oscillation between CPSS and RPSS, are provided as follows. For case 1 in Figure 10, both CPSS and RPSS are capable of damping the oscillation effectively. In cases 2 and 3 as shown in Figures 11 and 12 respectively, the stabilizing effect of CPSS is completely deteriorated. The speed difference severely oscillates and the system is unstable. On the other hand, the RPSS is successfully capable of damping out the oscillation. These study

TABLE 3. Eigenvalue and damping ratio of oscillation modes

Type of controller	Oscillation Mode	Eigenvalue	Damping ratio	Frequency (Hz)
No PSS	Inter-area	$-0.0629 \pm 3.9884i$	0.0158	0.6348
	Local 1	$-0.8625 \pm 6.9943i$	0.1224	1.1132
	Local 2	$-0.8609 \pm 7.2188i$	0.1184	1.1489
CPSS	Inter-area	$-0.6045 \pm 3.9756i$	0.1503	0.6327
	Local 1	$-2.3531 \pm 8.0122i$	0.2818	1.2752
	Local 2	$-2.4355 \pm 8.3738i$	0.2793	1.3327
RPSS	Inter-area	$-0.6641 \pm 3.8952i$	0.1681	0.6199
	Local 1	$-0.8572 \pm 7.7094i$	0.1105	1.2270
	Local 2	$-2.1134 \pm 9.4107i$	0.2191	1.4978

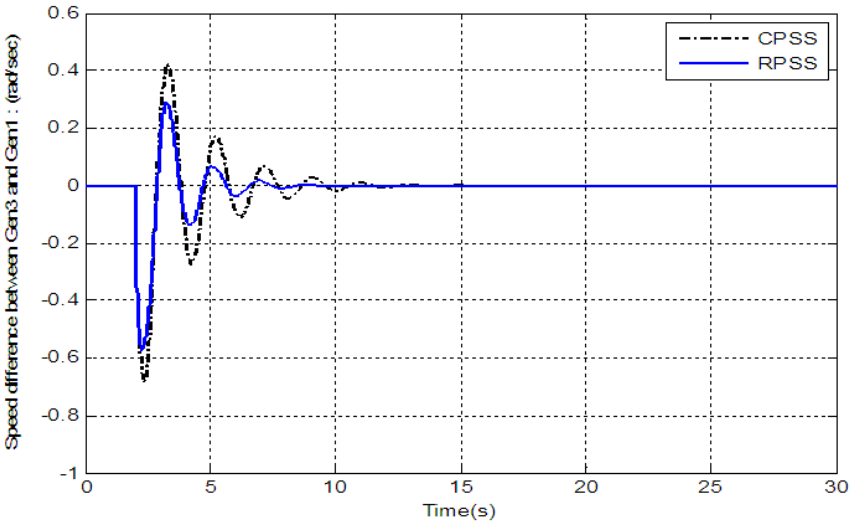

FIGURE 10. Speed difference between G3 and G1 in case 1

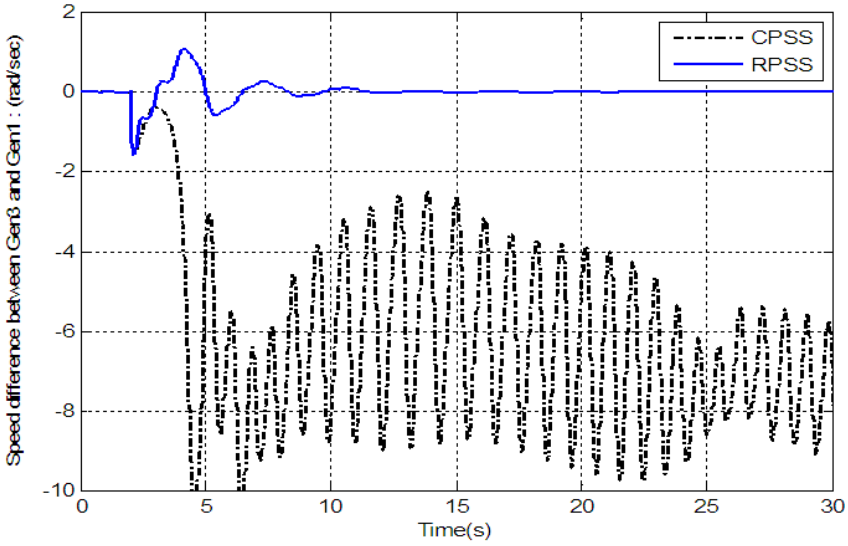

FIGURE 11. Speed difference between G3 and G1 in case 2

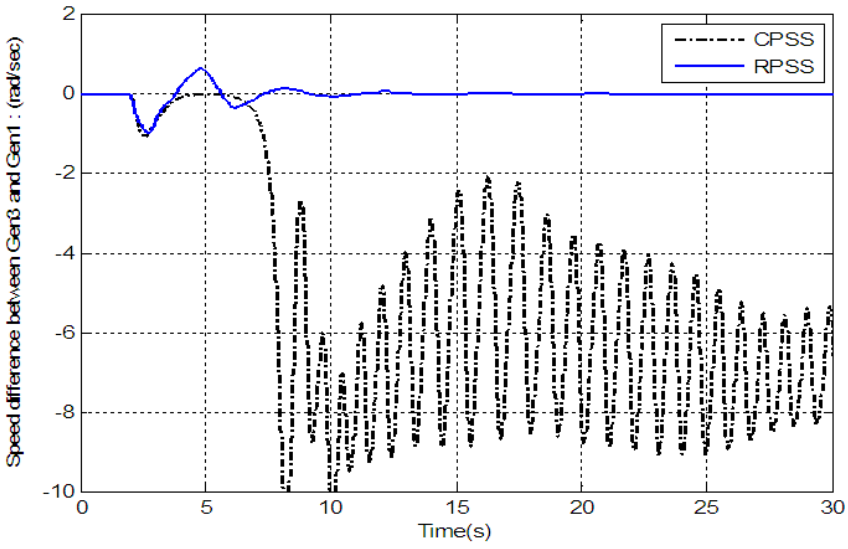

FIGURE 12. Speed difference between G3 and G1 in case 3

results confirm that the performance and robustness of the proposed RPSS are much superior to those of the CPSS.

For the case of varying time delay from 100-160 ms of RPSS as illustrated in Figure 13, simulation under the event of case 3 at the power flow 4.0 p.u. is performed. It can be observed that the speed difference at any time delay is almost the same response unless the time delay is 160 ms. It can be seen that a small oscillation occurs, the system is still stable. Therefore, RPSS is very robust against the time delay uncertainties.

4. **Application 2: Wide Area Robust Centralized TCSC Design.** In this part, the proposed method is applied to design the PSDC of TCSC which is connected in series with the transmission line between bus 7 and bus 8 as shown in Figure 14. By control of a capacitive reactance of TCSC, the power flow in a tie-line can be controlled directly

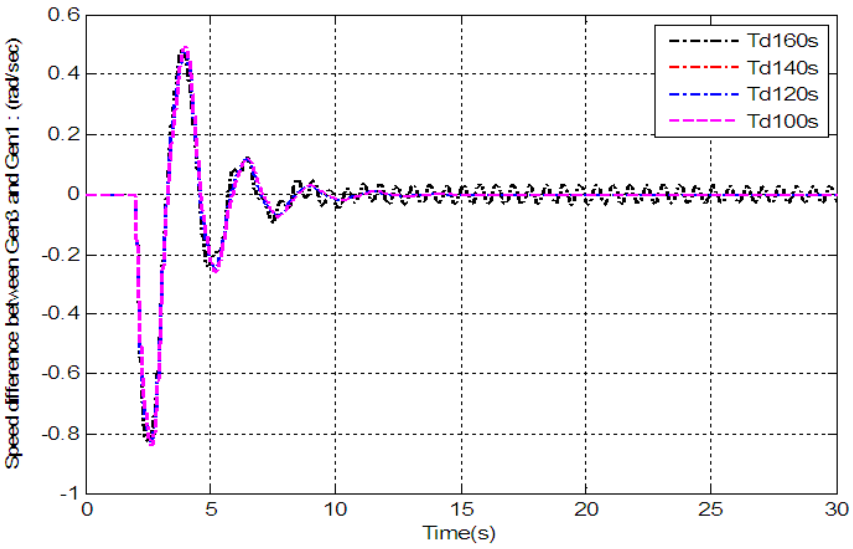

FIGURE 13. Speed difference between G3 and G1 of RPSS when the time delay is varied

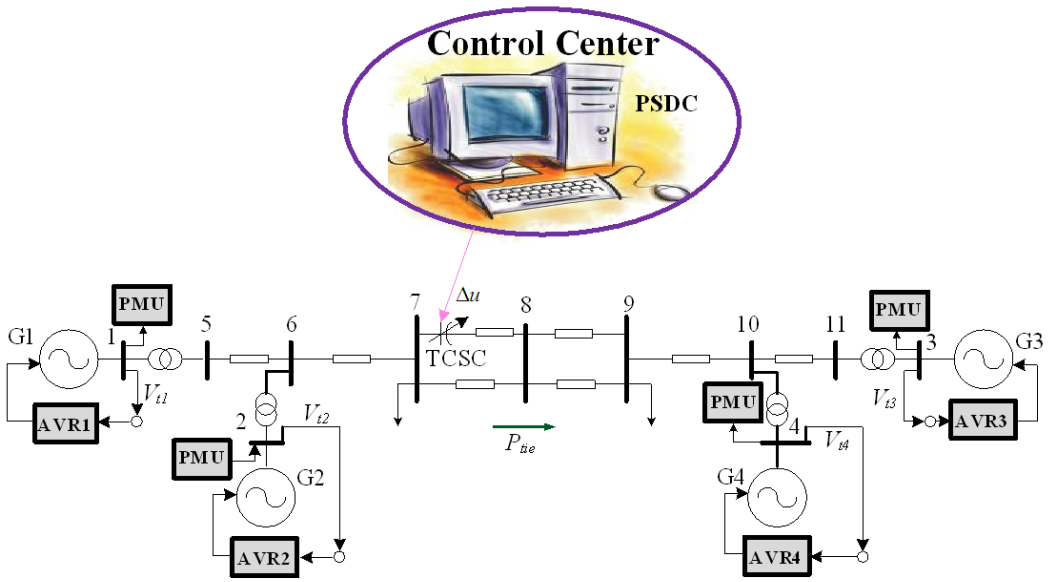

FIGURE 14. Wide area stabilization by TCSC

so that the inter-area power oscillation can be stabilized. Here, the TCSC is modeled by a variable series capacitor [18]. The block diagram of PSDC in Figure 3 can be applied for TCSC. The input signal is the speed difference between G1 and G3 while the output signal is the susceptance (B). The maximum and minimum limits of output signal are $B_{\max} = +0.033$ and $B_{\min} = -0.033$ p.u. (30% compensation of line reactance between bus 7 and 8). There are 5 control parameters of PSDC to be optimized by the proposed method.

First the model reduction is carried out by balanced realization. As a result, the original 33rd order system is reduced to 7th order system. As shown in Table 4, the eigenvalues corresponding to the inter-area oscillation mode of 7th and full order systems have almost the same values. Besides, the bode plots of 7th order and the full order systems are

TABLE 4. Comparison of eigenvalue of inter-area mode between reduced and full order models

Type of model	Eigenvalue (Inter-area mode)	Damping ratio	Frequency (Hz)
7th order	$-0.11626 \pm 3.82613i$	0.03037	0.6089
Full order	$-0.11623 \pm 3.82620i$	0.03036	0.6090

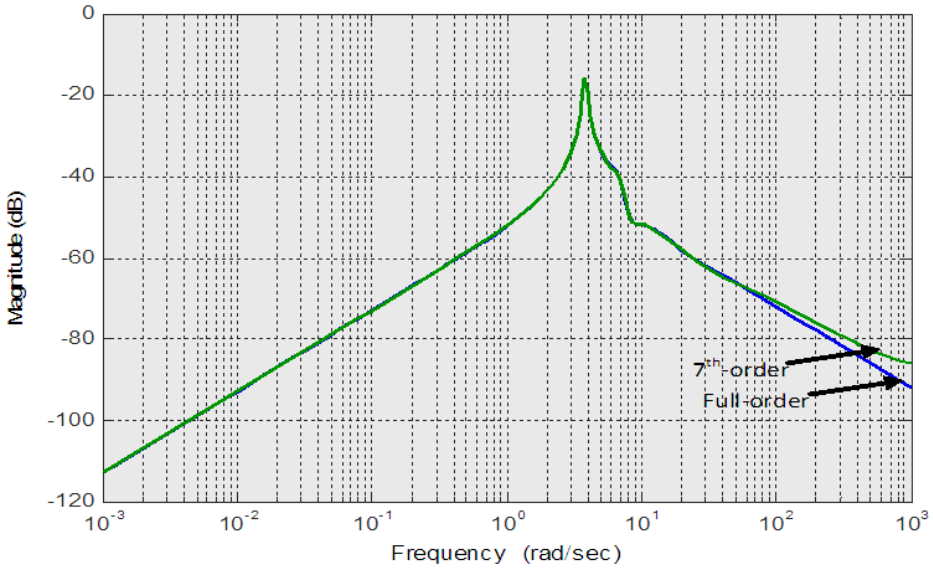

FIGURE 15. Bode plot of 7th-oder and full order systems

illustrated in Figure 15. The peak resonance of both bode plots occurs at about 3.8 rad/s. This frequency is consistent with the imaginary part of the eigenvalue. Here, the 7th order system is chosen for PSDC design.

Based on the operating conditions at $P_{tie} = 3$ p.u. and total time delay $(\tau_{d1} + \tau_{d2}) = 0.4$ s, the designed robust PSDC of TCSC which is referred to "RTCSC", is obtained as

$$\text{RTCSC} \qquad K_{RTCSC}(s) = 4.4348 \frac{(1 + 0.7628s)}{(1 + 0.5389s)} \frac{(1 + 0.7062s)}{(1 + 0.1590s)} \tag{18}$$

The robustness of RTCSC is compared with the TCSC designed without considering the robustness which is referred as "CTCSC". Note that, CTCSC is designed in the detailed linear model including the time delay to yield the same damping ratio and real part of the dominant modes as the design specification of RTCSC. The optimization problem of CTCSC based on the pole assignment is formulated as

$$\begin{array}{ll} \text{Minimize} & |\zeta_{spec} - \zeta| + |\sigma_{spec} - \sigma| \\ \text{Subject to} & K_{i,\min} \le K_i \le K_{i,\max}, \\ & T_{ij,\min} \le T_{ij} \le T_{ij,\max}, \quad i = 1, \quad j = 1, \ldots, 4 \end{array} \tag{19}$$

Solving (19) by PSO, the CTCSC is obtained as

$$\text{CTCSC} \qquad K_{CTCSC}(s) = 6.7688 \frac{(1 + 0.7001s)}{(1 + 0.3056s)} \frac{(1 + 0.5828s)}{(1 + 0.3383s)} \tag{20}$$

Table 5 shows the eigenvalue and damping ratio of dominant inter-area oscillation modes. Without TCSC, the damping ratio of oscillation mode is very poor. On the other

hand, the damping ratio and the real part of oscillation modes are achieved as the desired specification by both CTCSC and RTCSC.

Applying the designed CTCSC and RTCSC to the power system with full detailed linear model, Figure 16 shows the locus plot of oscillation modes in case of the system with either CTCSC or RTCSC when time delay is varied from 0.2-0.8 s. The inter-area mode in case of CTCSC tends to move to the unstable region when the time delay increases. In contrast, the RTCSC is able to stabilize the inter-area mode even at the large time delay.

TABLE 5. Eigenvalue and damping ratio of oscillation modes

Type of controller	Eigenvalue	Damping ratio	Frequency (Hz)
No TCSC	$-0.1321 \pm 3.9016i$	0.0338	0.6210
CTCSC	$-0.4016 \pm 4.1821i$	0.0956	0.6656
RTCSC	$-0.3989 \pm 4.0178i$	0.0988	0.6395

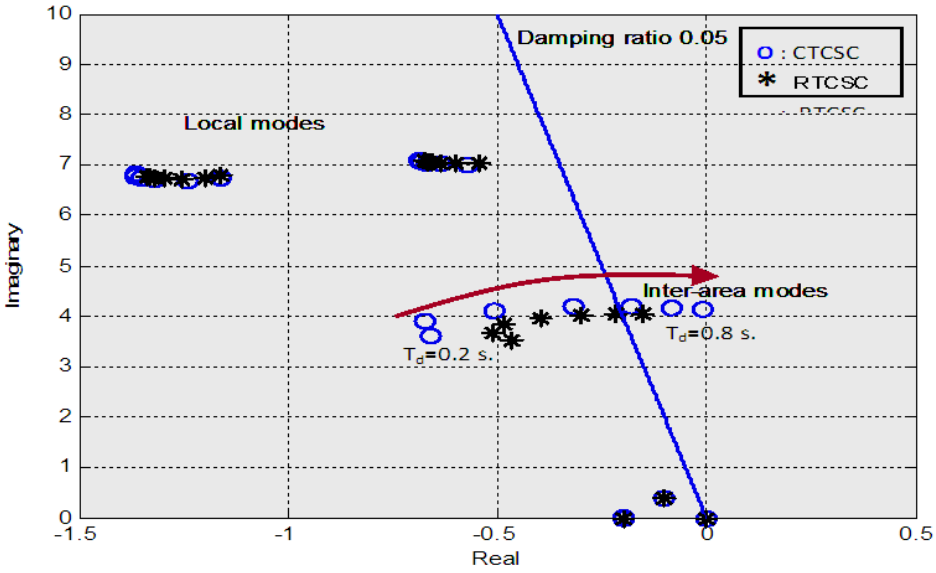

FIGURE 16. Locus of inter-area mode when time delay is varied from 0.2-0.8 s

TABLE 6. Case studies (MVA base = 100 MVA)

Case	Event	P_{tie} (p.u.)	Time delay(s)
1	A 3 phase fault occurs at one line between bus 8 and bus 9 at time = 2.0 s. The faulted line is opened at time = 2.05 s and re-closed at = 6.0 s.	4.0	0.4
2	A temporary 3 phase fault at bus 8 at time = 2.0 s for 50 ms. The fault is cleared naturally.	4.0	0.7
3	One line between bus 7 and bus 8 (without installed TCSC) is opened at time = 2.0 s and not re-closed.	4.0	0.7

Next, nonlinear simulations of three case studies under applied disturbances as given in Table 6 are performed. The comparisons of the phase difference between buses 7 and 9 which represents the inter-area oscillation between CTCSC and RTCSC are provided as follows. In case 1, as shown in Figure 17 the oscillation can be damped out by either CTCSC or RTCSC. In case 2, as depicted in Figure 18, the damping effect of CTCSC is much less than that of RTCSC. The TCSC is sensitive to the large time delay. For case 3 in Figure 19, the damping effect of CTCSC is completely deteriorated. The output of CTCSC hits the upper and lower limits. The power oscillation is severe and the system becomes unstable. On the other hand, the RTCSC is successfully capable of damping out the oscillation. The RTCSC is very robust against the large time delay. The power oscillation can be stabilized robustly.

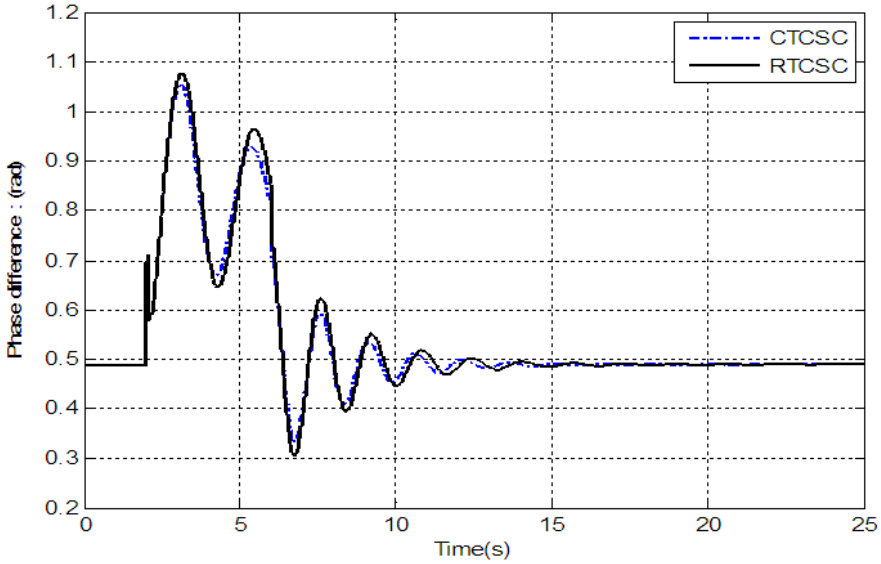

(a) Phase difference

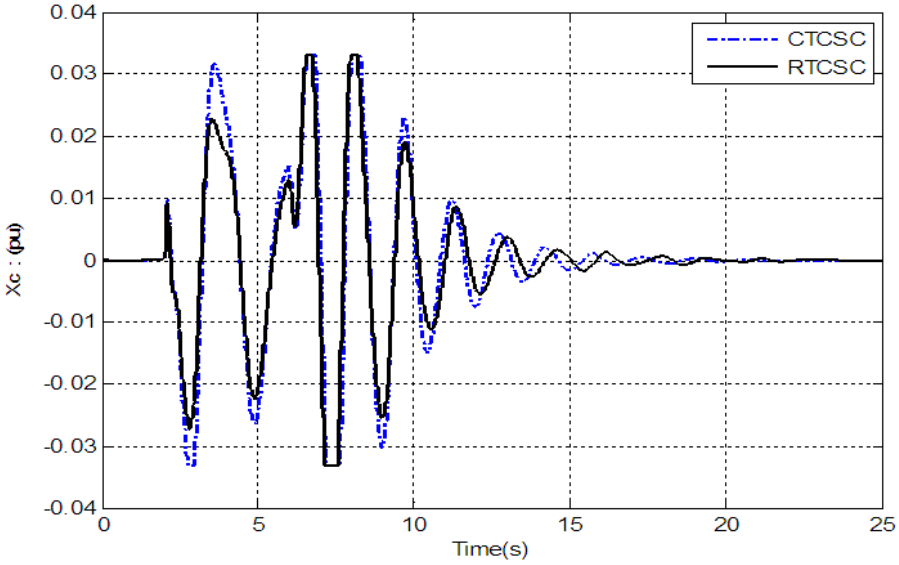

(b) Output of TCSC

FIGURE 17. Phase difference in case 1 with $T_d = 0.4$ s

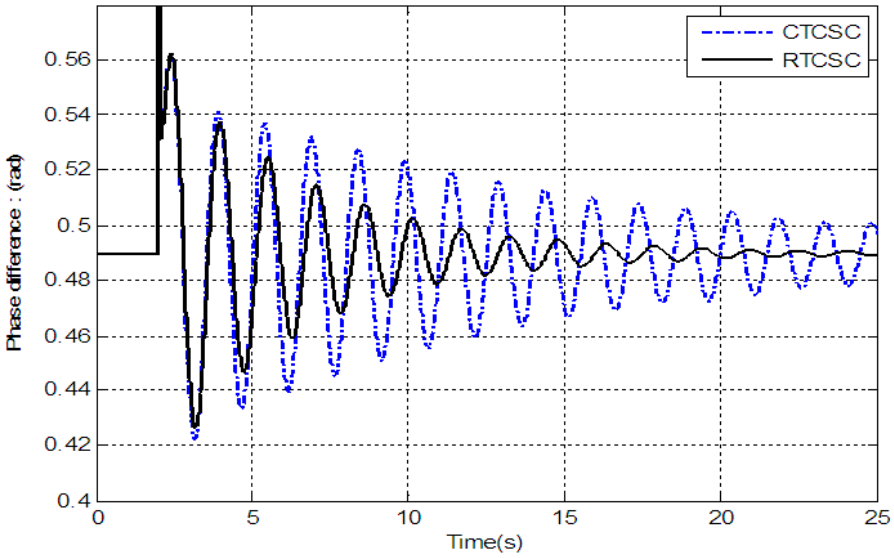

(a) Phase difference

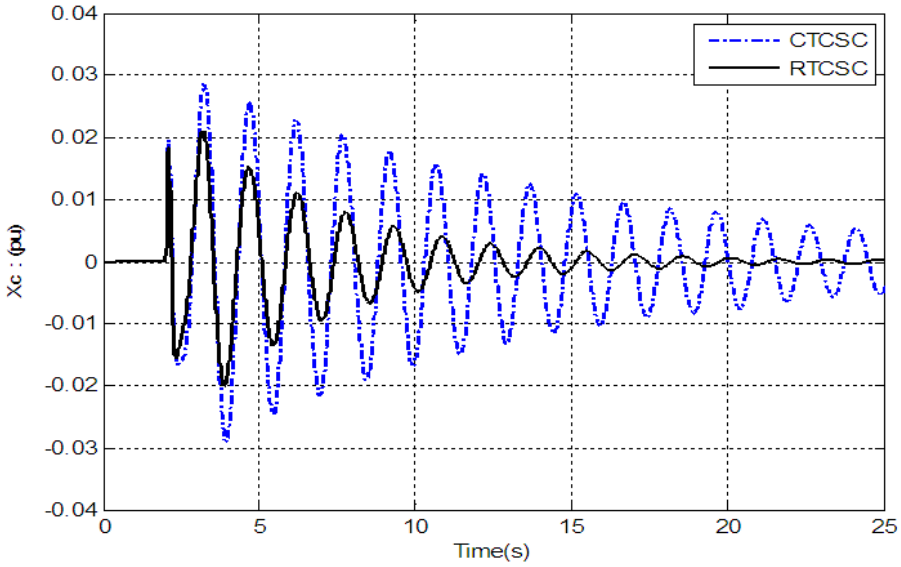

(b) Output of TCSC

FIGURE 18. Phase difference in case 2 with $T_d = 0.7$ s

5. **Conclusions.** The wide area robust centralized PSO-based specified structure H_∞ PSDC design taking uncertainties due to communication delay and system parameters into account is proposed in this paper. Without exact mathematical representation, the unstructured uncertainties due to time delay and system parameters are represented by the inverse input multiplicative model. The practical 2nd order lead/lag compensator is specified to be the structure of PSDC. The PSO is applied to automatically tune the control parameters based on the enhancement of damping effect and robust stability margin. Two examples of the robust centralized PSDC designed by the proposed technique, i.e., PSS and TCSC are demonstrated in a two-area four-machine interconnected power system. Simulation results show that the stabilizing effect and robustness of the proposed

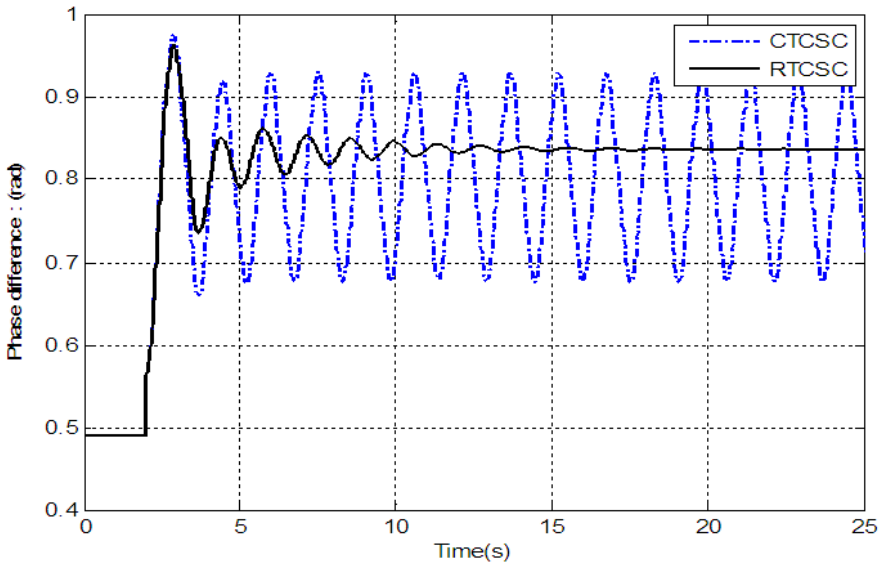

(a) Phase difference

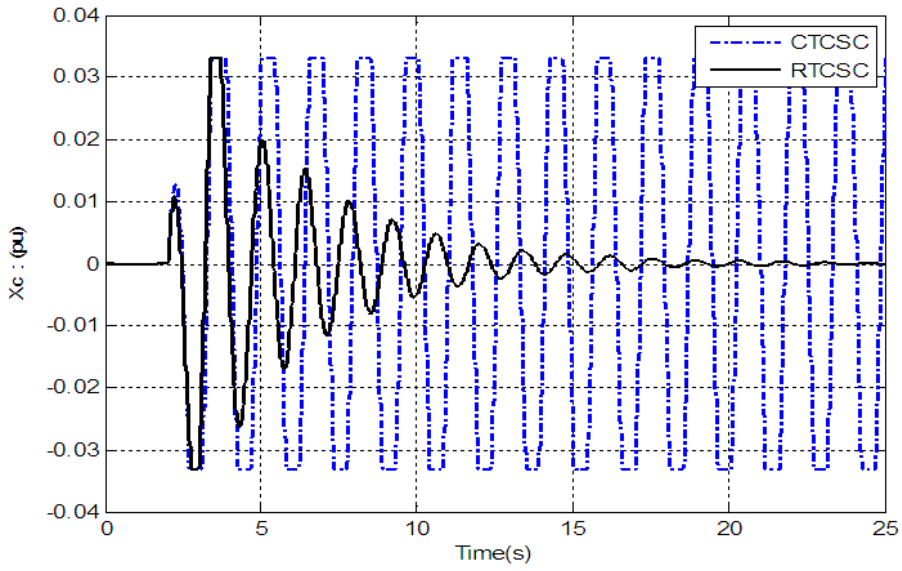

(b) Output of TCSC

FIGURE 19. Phase difference in case 3 with $T_d = 0.7$ s

robust centralized PSDC is much superior to those of the conventional centralized PSDC under severe disturbances, heavy power flow levels and variations of time delay and system parameters.

Acknowledgment. This work was supported by the King Mongkut's Institute of Technology Ladkrabang Research Fund.

REFERENCES

[1] G. Rogers, *Power System Oscillations*, Kluwer Acaemic, 2000.
[2] P. Kundur, *Power System Stability and Control*, McGraw-Hill, 1994.

[3] M. M. Al-Harthi, Robust AVR design based on mixed H_2/H_∞ pole placement using linear matrix inequality (LMI), *ICIC Express Letters*, vol.4, no.3(B), pp.963-971, 2010.
[4] L.-Y. Sun, J. Zhao and G. M. Dimirovski, Nonlinear robust controller design for thyristor controlled series compensation, *International Journal of Innovative Computing, Information and Control*, vol.5, no.4, pp.981-989, 2009.
[5] A. G. Phadke and T. S. Thorp, *Synchronized Phasor Measurements and Their Applications*, Springer, 2008.
[6] D. Karlsson, M. Hemmingsson and S. Lindahl, Wide area system monitoring and control, *IEEE Power & Energy Magazine*, vol.2, no.5, pp.68-76, 2004.
[7] I. Kanwa, R. Grondin and Y. Hebert, Wide area measurement based stabilizing control of large power systems – A decentralized/hierarchical approach, *IEEE Transactions on Power Systems*, vol.16, no.1, pp.136-153, 2001.
[8] H. Wu, K. S. Tsakalis and G. T. Heydt, Evaluation of time delay effects to wide area power system stabilizer design, *IEEE Transactions on Power Systems*, vol.19, no.4, pp.1935-1941, 2004.
[9] D. Dotta, A. S. Silva and I. C. Decker, Wide area measurements-based two-level control design considering signal transmission delay, *IEEE Transactions Power Systems*, vol.24, no.1, pp.208-216, 2009.
[10] T. Zabaiou, F. Okou, L. A. Dessaint and O. Akhrif, Time-delay compensation of a wide area measurements-based hierarchical voltage and speed regulator, *Canadian Journal of Electrical and Computer Engineering*, vol.33, no.2, pp.77-85, 2008.
[11] C.-Y. Chen and G. T.-C. Chiu, H_∞ robust controller design of media advance systems with time domain specifications, *International Journal of Innovative Computing, Information and Control*, vol.4, no.4, pp.813-828, 2008.
[12] S. Kaitwanidvilai, P. Olarnthichachart and I. Ngamroo, Weight optimization and structure specified robust H_∞ loop shaping control of a pneumatic servo system using genetic algorithm, *International Journal of Robotics and Automation*, vol.25, no.3, pp.229-239, 2010.
[13] J. W. Stahlhut, T. J. Browne, G. T. Heydt and V. Vittal, Latency viewed as a stochastic process and its impact on wide area power system control signals, *IEEE Transactions on Power Systems*, vol.23, no.1, pp.84-91, 2008.
[14] A. C. Antoulas, *Approximation of Large-Scale Dynamical Systems*, SIAM, 2005.
[15] S. Skogestad and I. Postlethwaite, *Multivariable Feedback Control: Analysis and Design*, John Wiley and Sons Ltd., 2005.
[16] B. Birge, PSOt – A particle swarm optimization toolbox for use with Matlab, *Proc. of Swarm Intelligence Symposium*, pp.182-186, 2003.
[17] J. Pahasa and I. Ngamroo, PSO based kernel principal component analysis and multi-class support vector machine for power quality problem classification, *International Journal of Innovative Computing, Information and Control*, vol.8, no.3(A), pp.1523-1539, 2012.
[18] N. G. Hingorani and L. Gyugyi, *Understanding FACTS: Concepts and Technology of Flexible AC Transmission Systems*, Wiley-IEEE, 1999.
[19] Y. Li, C. Rehtanz, D. Yang, S. Ruberg and U. Hager, Robust high-voltage direct current stabilizing control using wide area measurement and taking transmission time delay into consideration, *Proc. of IET Generation, Transmission & Distribution*, vol.5, no.3, pp.289-297, 2011.
[20] B. K. Lee, Y. H. Chen and B. S. Chen, Robust H_∞ power control for CDMA cellular communication systems, *IEEE Transactions on Signal Processing*, vol.54, no.10, pp.3947-3956, 2006.
[21] A. Cuenca, J. Salt, A. Sala and R. Piza, A delay-dependent dual-rate PID controller over and ethernet network, *IEEE Transactions on Industrial Informatics*, vol.7, no.1, pp.18-29, 2011.
[22] Y. Shi and B. Yu, Robust mixed H_2/H_∞ control of networked control systems with random time delays in both forward and backward communication links, *Automatica*, vol.47, no.4, pp.754-760, 2011.

Appendix. The power system model considering communication delay and system uncertainties can be derived as follows. At the nominal operating condition, the power system model is represented by

$$\dot{x} = Ax + Bu \tag{A1}$$

$$y = Cx \tag{A2}$$

where x is the state vector, u is the input vector, y is the output vector, A is the system matrix, B is the input matrix and C is the output matrix. When the system operating condition changes from the normal point, the system model can be described by

$$\dot{x} = (A + \Delta_a)x + (B + \Delta_b)u \tag{A3}$$

$$y = (C + \Delta_c)x \tag{A4}$$

where Δ_a, Δ_b and Δ_c are the system uncertainty associated with matrix A, B and C. Thus (A3) and (A4) can be rewritten as

$$\dot{x} = (I + \Delta_A)Ax + (I + \Delta_B)Bu \tag{A5}$$

$$y = (I + \Delta_C)Cx \tag{A6}$$

where $\Delta_A = \Delta_a A^{-1}$, $\Delta_B = \Delta_b B^{-1}$ and $\Delta_C = \Delta_c C^{-1}$. Equations (A5) and (A6) can be represented in the frequency domain by

$$G_u(s) = (I + \Delta_C)\, C \left\{sI - (I + \Delta_A)\, A\right\}^{-1} (I + \Delta_B)\, B \tag{A7}$$

where $G_u(s)$ is the transfer function of power system included with system uncertainties. Equation (A7) is rearranged by expressing the middle term in the multiplied form as

$$G_u(s) = (I + \Delta_C)\, C \left\{[I + \Delta'_A]\, [sI - A]\right\}^{-1} (I + \Delta_B)\, B \tag{A8}$$

where $\Delta'_A = -\Delta_A A[sI - A]^{-1}$. Equation (A8) can be rewritten as

$$G_u(s) = (I + \Delta_C)\, C\, [sI - A]^{-1}\, [I + \Delta_{AB}]\, B \tag{A9}$$

where $[I + \Delta_{AB}] = [I + \Delta'_A]^{-1}\, [I + \Delta_B]$, $[I + \Delta_{AB}]$ is the system uncertainty which is associated with matrices A and B. Equation (A9) can be rearranged so that

$$G_u(s) = (I + \Delta_{AB1})\, (I + \Delta_C) \left\{C\, [sI - A]^{-1}\, B\right\} (I + \Delta_{AB2}) \tag{A10}$$

or

$$G_u(s) = (I + \Delta_{ABC1}) \underbrace{\left\{C\, [sI - A]^{-1}\, B\right\}}_{G(s)} (I + \Delta_{AB2}) \tag{A11}$$

where $G(s)$ is the transfer function of the nominal system and $(I + \Delta_{ABC1}) = (I + \Delta_{AB1})$ $(I + \Delta_C)$. $(I + \Delta_{AB1})$ and $(I + \Delta_{AB2})$ can be calculated if either term is given. For example, if $(I + \Delta_{AB2})$ is given, $(I + \Delta_{AB1})$ can be calculated by

$$(I + \Delta_{AB1}) = G_u(s) \cdot \left[(I + \Delta_C)\, C\, [sI - A]^{-1}\, B\, (I + \Delta_{AB2})\right]^{-1} \tag{A12}$$

When the uncertainty due to communication delay is taken into account, the system equation considering both system and communication delay uncertainties ($G_P(s)$) can be expressed by

$$\begin{aligned} G_p(s) &= e^{-(T_{d1} + \Delta_{T_{d1}})s} \cdot G_u(s) \cdot e^{-(T_{d2} + \Delta_{T_{d2}})s} \\ &= e^{-\Delta_{T_{d1}} s} \left\{e^{-T_{d1} s} \cdot G_u(s) \cdot e^{-T_{d2} s}\right\} e^{-\Delta_{T_{d2}} s} \end{aligned} \tag{A13}$$

where T_{d1} and T_{d2} are the transmitted and received communication time delay, respectively. $\Delta_{T_{d1}}$ and $\Delta_{T_{d2}}$ are the uncertainty of transmitted and received communication time delay, respectively.

The uncertainty of time delay terms $e^{-\Delta_{T_{d1}} s}$ and $e^{-\Delta_{T_{d2}} s}$ can be expressed in another form as $(I + \Delta_{d1})$ and $(I + \Delta_{d2})$. This can be derived as follows.

Substituting $s = \sigma + j\omega$ into $e^{-\Delta_{T_{d1}} s}$ gives

$$e^{-\Delta_{T_{d1}} s} = e^{-\Delta_{T_{d1}}(\sigma + j\omega)} = e^{-\sigma \Delta_{T_{d1}}} \angle - \omega \Delta_{T_{d1}} = 1 + \left[(e^{-\sigma \Delta_{T_{d1}}} \angle - \omega \Delta_{T_{d1}}) - 1\right] = 1 + T_{d1}$$

where $T_{d1} = \left[(e^{-\sigma \Delta_{T_{d1}}} \angle - \omega \Delta_{T_{d1}}) - 1\right]$. The term $e^{-\Delta_{T_{d2}} s}$ can also be represented in the same way. Since $G_p(s) = e^{-\Delta_{T_{d1}} s} \cdot I \left\{e^{-T_{d1} s} \cdot G_u(s) \cdot e^{-T_{d2} s}\right\} I \cdot e^{-\Delta_{T_{d2}} s}$, then to substitute

$e^{-\Delta_{T_{d1}} s} \cdot I$ and $I \cdot e^{-\Delta_{T_{d2}} s}$ in (A13) by $(I + \Delta_{d1})$ and $(I + \Delta_{d2})$, respectively and express Δ_{d1} and Δ_{d2} by $T_{d1} \cdot I$ and $T_{d2} \cdot I$ respectively, yields

$$\begin{aligned} G_p(s) &= (I + \Delta_{d1}) \left\{ e^{-T_{d1} s} \cdot G_u(s) \cdot e^{-T_{d2} s} \right\} (I + \Delta_{d2}) \\ &= (I + \Delta_{d1}) \left\{ (I + \Delta_{ABC1}) \underbrace{\left\{ e^{-T_{d1} s} \cdot C \left[sI - A \right]^{-1} B \cdot e^{-T_{d2} s} \right\}}_{G'(s)} (I + \Delta_{AB2}) \right\} (I + \Delta_{d2}) \\ &= (I + \Delta_1) \underbrace{\left\{ e^{-T_{d1} s} \cdot C \left[sI - A \right]^{-1} B \cdot e^{-T_{d2} s} \right\}}_{G'(s)} (I + \Delta_2) \end{aligned} \tag{A14}$$

where $G'(s)$ is the nominal plant model included with communication delay, $(I + \Delta_1) = (I + \Delta_{d1})(I + \Delta_{ABC1})$ and $(I + \Delta_2) = (I + \Delta_{AB2})(I + \Delta_{d2})$. To calculate the robust stability margin, $(I + \Delta_1)$ and $(I + \Delta_2)$ can be rewritten in the inverse form as

$$G_p(s) = (I - \Delta_{M1})^{-1} \underbrace{\left\{ e^{-T_{d1} s} \cdot C \left[sI - A \right]^{-1} B \cdot e^{-T_{d2} s} \right\}}_{G'(s)} (I - \Delta_{M2})^{-1} \tag{A15}$$

where $(I - \Delta_{M1})^{-1} = (I + \Delta_1)$ and $(I - \Delta_{M2})^{-1} = (I + \Delta_2)$, Δ_{M1} is the inverse input multiplicative perturbation which represents uncertainties of both system parameters and transmitted time delay, Δ_{M2} is the inverse output multiplicative perturbation which represents uncertainties of both system parameters and received time delay. Equation (A15) can be shown by the block diagram in Figure 4.